Available online at www.sciencedirect.com
SCIENCE DIRECT®
ELSEVIER
Journal of Nuclear Materials 337–339 (2005) 391–394
journal of nuclear materials
www.elsevier.com/locate/jnucmat

Comparison of plasma parameters between QH and ELMing phases of the same discharges

C.J. Lasniera [a,*], W.P. West [b], K.H. Burrell [b], J.S. deGrassie [b], E.J. Doyle [c], T.H. Osborne [b]

[a] *Lawrence Livermore National Laboratory, P.O. Box 808, L-637, Livermore, CA 94551, USA*
[b] *General Atomics, San Diego, CA 92186-5608, USA*
[c] *University of California, Los Angeles, CA 90095-1597, USA*

Abstract

H-mode confinement is observed for many energy confinement times without edge localized modes (ELMs) in QH (quiescent high-confinement)-mode discharges in DIII–D. To determine the critical differences between ELMing and QH modes we compared electron temperature (T_e), density (n_e), and ion temperature (T_i), in the pedestal (ped) and scrape-off layer (SOL) for a group of discharges. We also compared the electron pressures P_{ped}, and maximum pressure gradient $\nabla^{max} P_{e,ped}$ because of their importance in confinement and stability. Experimental results show that the core line averaged density, median $T_{e,ped}$, $T_{e,SOL}$, and $T_{e,ped}$ width, and $T_{i,SOL}$ are nearly the same in QH mode as that during ELMs. The $n_{e,ped}$ (average), $n_{e,ped}$ width, P_{ped}, and $\nabla^{max} P_{e,ped}$ are similar to corresponding values in QH mode and at various times between ELMs. However, the median $T_{i,ped}$ is 1.6 times higher in QH mode than during ELMing.

PACS: 52.40.H; 52.55
Keywords: DIII–D; Divertor; Edge pedestal; SOL plasma boundary

1. Introduction

This paper presents a statistical comparison of several important plasma parameters in QH-mode and ELMing H-mode. Quiescent high confinement (QH) mode is exhibited in DIII–D tokamak plasmas with H-mode confinement, long periods with no edge localized modes (ELMs), and quasi-stationary plasma parameters [1–4]. QH-mode has been seen in ASDEX-U [5], JET [6], and JT60-U [7] and is of interest for avoiding ELM-induced damage to the divertors of future large tokamaks. Observed requirements for QH-mode include neutral beams injected opposite to the plasma current, relatively low plasma density, and a large gap between the outer wall and the plasma separatrix (g_{out}). The edge n_e and T_e profiles in QH-mode are similar to those of H-mode [8].

We examine time slices from a group of discharges exhibiting both QH and ELMingH-mode behavior, and compare the plasma parameters between the two modes for different times during the ELM cycle. The discharges have been selected with nearly the same toroidal field (2.0 ± 0.05 T), plasma current (1.3 ± 0.05 MA), and upper single-null magnetic configuration. The ion temperature data have been further selected for 9.5 cm < g_{out} < 10.5 cm.

* Corresponding author.
E-mail address: lasnier@llnl.gov (C.J. Lasniera).

0022-3115/$ - see front matter © 2004 Elsevier B.V. All rights reserved.
doi:10.1016/j.jnucmat.2004.10.059

2. Procedure

Nearly all the QH discharges exhibit ELMing H-mode at some time during the pulse, often shortly after the neutral beam counter-injection begins. ELMing was often followed by a transition to quiescent behavior at the same confinement and nearly the same density. The plasma parameters analyzed include: electron pedestal (ped) and scrape-off layer (SOL) quantities: $T_{\mathrm{e,ped}}$ and $n_{\mathrm{e,ped}}$, $T_{\mathrm{e,ped}}$ and $n_{\mathrm{e,ped}}$ width, $T_{\mathrm{e,SOL}}$, $n_{\mathrm{e,SOL}}$, $T_{\mathrm{i,ped}}$, $T_{\mathrm{i,SOL}}$, maximum electron pressure gradient ($\nabla^{\max}P_{\mathrm{e,ped}}$), and electron pedestal pressure ($P_{\mathrm{e,ped}}$). The ion temperatures were obtained from charge-exchange recombination spectra of carbon. Electron temperature and density profiles were obtained using modified hyperbolic tangent fits to Thomson scattering data [9]. The SOL value used was from the far SOL part of this fit. Electron pressure was calculated from the product of the electron density and temperature. The maximum electron pressure gradient was from the analytic derivative of the modified hyperbolic tangent.

The QH-mode data were treated as a single group, and statistics of the plasma parameters were obtained. The ELM electron data were separated into groups by ELM phase and the statistics for each phase were determined. The ELM phase is defined as the time since the last ELM divided by the time between the last ELM and next ELM peak in D_α, as measured at the outer midplane. For these discharges, the time resolution of the ion temperature data is not sufficient to separate it by ELM phase, so T_{i} is considered in one group averaged over ELM phase.

In the figures, square symbols represent the median value of a quantity during ELMing at a particular ELM phase, circles are the average value, and a band depicts the median QH value. The height of the band represents the error bar. Some of the figures use a suppressed zero to better illustrate small variations. The size of all error bars is $\sigma/\sqrt{n}$ where σ is the standard deviation of the sampled quantity and n is the number of samples.

The median value is included since the mean can be strongly biased by a few outlying points. In cases where the behavior of the mean is similar to that of the median, we can say with more confidence that the behavior is typical.

3. Results

3.1. Electron temperature

Immediately after an ELM, the $T_{\mathrm{e,ped}}$ drops 10–15% and then recovers its pre-ELM value before the next ELM. The QH-mode pedestal median electron temperature is slightly (4%) higher than in any part of the ELMing phase (Fig. 1(a)).

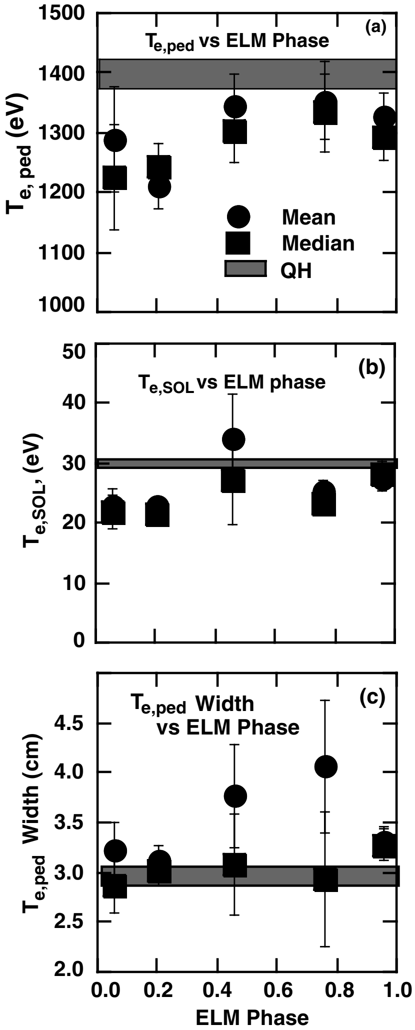

Fig. 1. (a) $T_{\mathrm{e,ped}}$ vs ELM phase, (b) $T_{\mathrm{e,SOL}}$ vs ELM phase, (c) $T_{\mathrm{e,ped}}$ width vs ELM phase. In this and succeeding figures, square symbols represent median values during ELMing, circles denote average values during ELMing, and the band represents the value during QH mode.

The electron temperature in the SOL shows a 25% drop after an ELM pulse, nearly twice the change in the pedestal. The QH value is nearly the same as the highest inter-ELM value (Fig. 1(b)). The median $T_{\mathrm{e,ped}}$ width is essentially unchanged during the ELM cycle (but the mean $T_{\mathrm{e,ped}}$ width rises), and is the same in the QH and ELMing phases (Fig. 1(c)).

3.2. Electron density

The median $n_{\mathrm{e,ped}}$ increases abruptly, then more gradually, after an ELM, until the next ELM, when it drops quickly (Fig. 2(a)). In this data set the highest value of $n_{\mathrm{e,ped}}$ is 35% more than the lowest $n_{\mathrm{e,ped}}$. The QH value

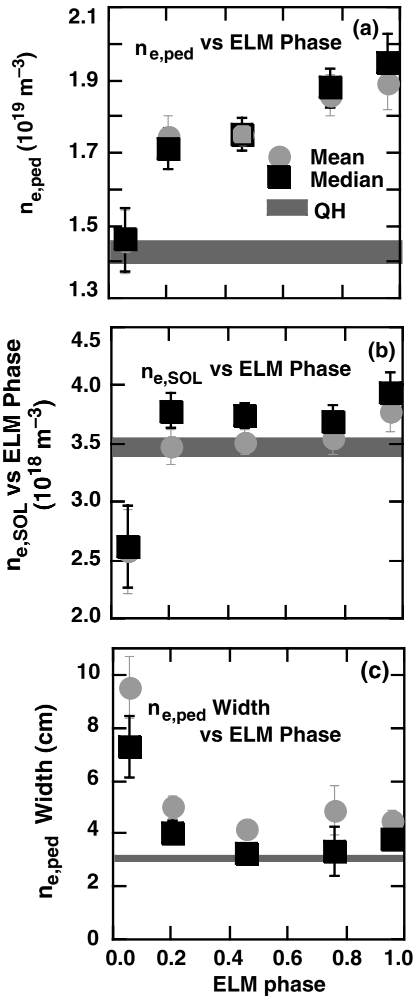

Fig. 2. (a) $n_{e,ped}$ vs ELM phase, (b) $n_{e,SOL}$ vs ELM phase, (c) $n_{e,ped}$ width vs ELM phase.

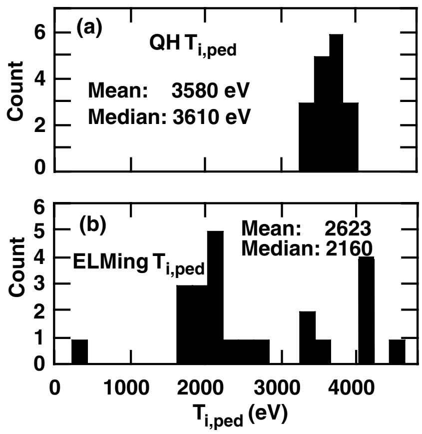

Fig. 3. (a) Histogram of $T_{i,ped}$ during QH-mode, (b) for ELMing.

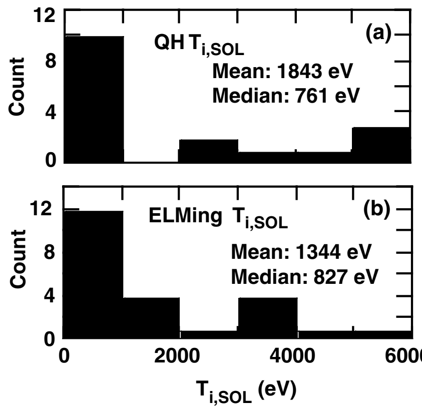

Fig. 4. (a) Histogram of $T_{i,SOL}$ during QH-mode, (b) for ELMing.

of $n_{e,ped}$ is nearly the same as the lowest value during ELMing, which occurs shortly after the ELM (ELM phase ~ 5%).

The SOL density drops at the time of an ELM pulse, then rises sharply to a plateau, which is held until the next ELM. The QH SOL density corresponds to the plateau level during ELMing (Fig. 2(b)).

The width of the electron density pedestal is largest immediately after an ELM, then decreases a factor of 2, reaching a plateau value until the next ELM. The width during QH-mode corresponds to the plateau level during ELMing (Fig. 2(c)).

3.3. Ion temperature

The median $T_{i,ped}$ is much higher in QH-mode than during ELMing (Fig. 3), by a factor of 1.6, even though similar densities, input power levels, and energy confinement occur in the two phases.

The $T_{i,SOL}$ is similar in QH-mode to that during ELMing (Fig. 4).

3.4. Electron pressure in the pedestal

The median $P_{e,ped}$ at the top of the pedestal (Fig. 5(a)) drops by ~40% shortly after an ELM, and recovers before the next ELM. The QH value of $P_{e,ped}$ is intermediate between these extremes. This supports the idea that in QH-mode the ELM is replaced by another mode, usually the continuous edge harmonic oscillation (EHO) [1–5] which appears to regulate the pedestal particle confinement and pedestal pressure.

The $\nabla^{max}P_{e,ped}$ shows a dramatic change over an ELM cycle. The ELMing $\nabla^{max}P_{e,ped}$ is 30% less steep than the QH-mode gradient immediately after an ELM

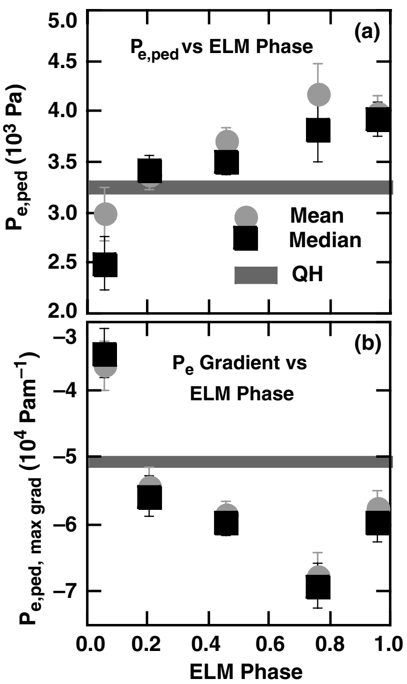

Fig. 5. (a) $P_{e,ped}$ vs ELM phase, (b) maximum gradient of $P_{e,ped}$ vs ELM phase.

pulse, steepens to the QH value at 15% ELM phase, then at later ELM phase reaches 40% steeper than the QH gradient. Clearly the continuous nature of the EHO maintains some average $\nabla^{max}P_{e,ped}$ in contrast to the ELMs, probably due to the EHO ejecting particles from the plasma.

4. Discussion

Each of the averaged parameters examined for the ELMing H-modes attains a similar value to QH-mode values at some particular ELM phase, although the precise timing differs for each parameter. The exception is T_i in the pedestal, which is consistently higher during QH-mode.

The $T_{e,ped}$, $T_{e,SOL}$, and $T_{e,ped}$ width, do not show a large difference from a constant ELM value in this data, within limits of the error bars. The value of $n_{e,ped}$ for QH-mode matches ELMing H-mode at an ELM phase of 5% and clearly does not match later ELM phases. The $n_{e,SOL}$ for QH-mode is close to ELMing n_e for ELM phase $\geqq$ 20%. The width of the n_e pedestal for QH-mode agrees with the ELMing value for ELM phases $\geqq$ 45%. Both the $P_{e,ped}$ and $\nabla^{max}P_{e,ped}$ for QH-mode agree with ELMing H-mode for an ELM phase of 15%. The $T_{i,ped}$ values for QH-mode are 1.6 times the respective values in ELMing H-mode.

When averaged over ELM phase as the T_i data was, the $n_{e,ped}$ median value for ELMing H-mode is 20% higher than for QH-mode. This is significant, but less striking than the difference in pedestal ion temperatures.

The tempting conclusion is that the higher ion temperatures are responsible for producing QH-mode, although uncertainties in the data may not justify this, nor is this a complete examination of the plasma behavior. However, our results do place a constraint on any model seeking to explain QH-mode. Database work can be a useful guide, but does not take the place of detailed experimental comparisons. Within this set of discharges are a variety of plasma shapes, heating power, momentum input, edge current (not measured in this data set), and other variables. All have effects on the pedestal stability limit and transport. Nevertheless, the data in this paper indicate that QH mode parameters remain within the range of time variation for ELMs except for T_i. Possibly the difference in ion temperatures is caused by fast ions in QH mode, which may play a role in stabilizing the ELMs.

Acknowledgments

This work was supported by the US Department of Energy under W-7405-ENG-48, DE-FC02-04ER54698 and DE-FG03-01ER54615.

References

[1] K.H. Burrell et al., Phys. Plasmas 8 (2001) 2153.
[2] C.M. Greenfield et al., Phys. Rev. Lett. 86 (2001) 4544.
[3] W.P. West et al., Phys. Plasmas 9 (2002) 1970.
[4] W.P. West, K.H. Burrell, J.S. deGrassie, in: Proceedings of the 30th European Conference on Controlled Fusion and Plasma Physics, St. Petersburg, Russian Federation, European Physical Society, Geneva, 2003, CD-ROM.
[5] W. Suttrop et al., Plasma Phys. Control. Fus. 45 (2003) 1399.
[6] W. Suttrop, 2003, private communication.
[7] Y. Sakamoto, 2003, private communication.
[8] W.P. West et al., Plasma Phys. Control. Fus. 46 (2004) A179.
[9] R.J. Groebner, T.H. Osborne, Phys. Plasmas 5 (1998) 1800.